

1 **Rapeseed oleosomes facilitate intestinal lymphatic delivery**
2 **and oral bioavailability of cannabidiol**

3
4 Liuhang Ji¹, Wanshan Feng¹, Haojie Chen¹, YenJu Chu¹, Abigail Wong¹, Yufei Zhu¹,
5 Graziamarina Sinatra¹, Filippo Bramante², Frédéric Carrière³, Michael J. Stocks¹,
6 Vincenzo di Bari², David A. Gray², Pavel Gershkovich^{1,*}

7
8 ¹School of Pharmacy, University of Nottingham, Nottingham, NG7 2RD, UK
9 ²School of Biosciences, Sutton Bonington Campus, University of Nottingham,
10 Loughborough, Leicestershire LE12 5RD, UK
11 ³CNRS, Aix Marseille Université, UMR7281Bioénergétique et Ingénierie des
12 Protéines, 31 Chemin Joseph Aiguier, 13402, Marseille Cedex 20, France.

13
14 ***Corresponding author:**
15 Pavel Gershkovich, PhD
16 School of Pharmacy
17 University of Nottingham, University Park
18 Nottingham, UK
19 NG7 2RD
20 Tel: +44 (0) 115 846 8014
21 Fax: +44 (0) 115 951 3412
22 Email: pavel.gershkovich@nottingham.ac.uk

23
24
25
26
27
28
29
30
31
32
33
34
35
36
37
38
39
40

1 **Abstract**

2 Due to high lipophilicity and extensive first-pass metabolic loss, cannabidiol (CBD)
3 has low oral bioavailability. Co-administration of CBD and long-chain lipids facilitates
4 the intestinal lymphatic delivery, resulting in higher systemic bioavailability, as well as
5 high levels of the drug within the intestinal lymphatic system. However, despite
6 previous attempts with various lipid-based formulations, the oral bioavailability of
7 CBD is still limited. In this work, we have developed a novel formulation of CBD
8 based on natural rapeseed oleosomes. *In vivo* studies in rats demonstrated that oral
9 administration of CBD-loaded rapeseed oleosomes leads to substantially higher oral
10 bioavailability and intestinal lymphatic targeting of CBD in comparison with rapeseed
11 oil or artificial emulsion made of rapeseed oil and lecithin.

12 *In vitro* mechanistic assessments, including *in vitro* lipolysis and peroxide value
13 determination suggest that the lower oxidative state of the oil in oleosomes in
14 comparison to crude oil or artificial emulsion is likely to be the main factor responsible
15 for the superior performance of the CBD-loaded rapeseed oleosomes *in vivo*.

16 Although further investigation will be needed, the data suggest that natural seeds-
17 derived oleosomes can be used as a promising lipid-based drug delivery platform
18 promoting the bioavailability and lymphatic delivery of lipophilic drugs.

19

20

1 **Keywords:**

2 Cannabidiol, Intestinal lymphatic delivery, Lipid-based formulation, Rapeseed
3 oleosomes, Oral bioavailability

4

5

6

7

8

9

10

11

12

13

14

15

16

1 **Abbreviations**

2 AUC - Area Under Curve

3 BCS - Biopharmaceutical Classification System

4 BSU - Bio-Support Unit

5 CBD - Cannabidiol

6 DDT - Dichlorodiphenyltrichloroethane

7 HPLC - High-Performance Liquid Chromatography

8 MLN - Mesenteric Lymph Nodes

9 PC – Phosphatidylcholine

10 PDA - Photodiode Array Ultraviolet

11 SD - Standard Deviation

12 SDS - Sodium Dodecyl sulphate

13 TG - Triglycerides

14 CYP - Cytochrome P450

15

1. Introduction

Cannabidiol (CBD) is a highly lipophilic Biopharmaceutics Classification System (BCS) Class II phytocannabinoid originally isolated from the *Cannabis sativa* plant. According to previous reports, CBD has substantial immunomodulatory effects at high concentrations, suggesting its potential in treatment of autoimmune diseases (Hess et al., 2016; Hoffenberg et al., 2019; Nichols and Kaplan, 2019; Zgair et al., 2017). Efficient delivery of CBD to the intestinal lymphatic system can lead to sufficient exposure of the immune cells to the drug, potentially resulting in more efficient treatment of autoimmune diseases (Zgair et al., 2017). Moreover, enhanced systemic bioavailability of CBD could lead to benefits for patients affected by conditions such as epilepsy or cancer (Alice Brookes, 2024; Arzimanoglou et al., 2020; Chen et al., 2018; Seltzer et al., 2020). As reported previously, cannabidiol is metabolized by cytochrome P450 (CYP) enzymes (mainly by CYP3A4 and CYP2C19) and glucuronosyltransferases (minor contribution) in the liver (primarily) and intestinal wall (Court et al., 2024; Jiang et al., 2011; Perucca and Bialer, 2020). Due to the extensive first-pass metabolism and poor aqueous solubility, the oral bioavailability of CBD following oral administration is limited (Franco et al., 2020; Mechoulam et al., 2002; Perucca and Bialer, 2020).

It is reported that the oral bioavailability of CBD in fasting state in humans is as low as 6% (Franco et al., 2020; Perucca and Bialer, 2020). Co-administration of highly lipophilic drugs and long-chain triglycerides to facilitate the intestinal lymphatic drug

1 delivery is an effective strategy to improve the oral bioavailability (Kalepu et al., 2013;
2 Porter et al., 2007; Porter et al., 2013). Lipid-based formulations usually contain an
3 oil phase mixed or not with various types of surfactants to ensure dispersion of the oil
4 phase in the gastrointestinal tract contents (Porter et al., 2007). Both the initial
5 components of lipid-based formulations and their lipolysis products are important for
6 the intraluminal processing and absorption of the drug (Carrière, 2016). When long-
7 chain triglycerides enter the gastrointestinal tract, they will be enzymatically
8 hydrolysed to release fatty acids and monoglycerides. These lipid digestion products,
9 together with bile salts and phospholipids form mixed micelles, facilitate the diffusion
10 to the intestinal wall and eventually absorption into intestinal epithelial cells. In the
11 enterocytes, long-chain fatty acids and monoglycerides are re-esterified to
12 triglycerides and packed into chylomicrons. These large lipoproteins are then
13 transported into the intestinal lymphatic system and from there to the thoracic lymph
14 duct and systemic blood circulation, avoiding liver and hepatic first-pass metabolism
15 (Kalepu et al., 2013; Porter et al., 2007). Therefore, if a highly lipophilic drug with
16 appropriate physicochemical properties for affinity to chylomicrons is administered
17 together with long-chain triglycerides, higher systemic bioavailability and efficient
18 targeting into intestinal lymphatic system could be achieved, especially if the hepatic
19 first-pass metabolism was a primary limiting factor of the oral bioavailability.

20 We have shown previously that sesame oil facilitates the delivery of CBD to the
21 intestinal lymphatic system following oral administration in rats (Zgair et al., 2017). As
22 a result, CBD concentrations in lymph fluid could reach ~250 times higher levels than

1 in plasma, and systemic exposure was about 3-fold higher compared with lipid-free
2 formulations (Zgair et al., 2017). In a later study it was found that olive oil formulation
3 led to a similar extent of oral bioavailability and lymphatic delivery of CBD as sesame
4 oil, but with somewhat lower variability (Feng et al., 2022). Interestingly, even with
5 efficient intestinal lymphatic delivery of CBD associated with sesame or olive oil
6 formulations, the oral bioavailability of the drug was only about 20% (Feng et al.,
7 2022; Zgair et al., 2016). In our previous attempts to improve further the
8 bioavailability and lymphatic targeting of CBD, we have used pre-digested lipid
9 formulations, medium-chain triglycerides or surfactants, resulting in higher micellar
10 solubilisation of the drug *in vitro*, but natural vegetable oils still performed better than
11 these formulations *in vivo* (Feng et al., 2021a; Feng et al., 2021b). This could
12 potentially be due to existence of several minor constituents in natural oils, affecting
13 their stability and digestion efficiency (Feng et al., 2021a). Therefore, in this work we
14 have chosen to amend the approach of development of lipid-based formulations of
15 CBD, and instead of pre-digesting, or increasing the emulsification or micellar
16 solubilisation by various excipients, we have opted to use natural plant seeds-derived
17 oleosomes as a drug delivery vehicle (Romero-Guzmán et al., 2020). Oleosomes are
18 triglyceride (TG) storage organelles in plant seeds and consist of a triglyceride core
19 surrounded by a monolayer of phospholipids and proteins (De Chirico et al., 2018;
20 Romero-Guzmán et al., 2020). Although some *in vitro* studies assessed the potential
21 use of oleosomes as drug delivery vehicles (Cho et al., 2018), it is unknown if they
22 can indeed improve oral bioavailability and lymphatic delivery of CBD or other drugs.

1 Thus, the aim of this work is to test the hypothesis that natural rapeseed oleosomes
2 could increase the oral bioavailability and intestinal lymphatic delivery of CBD in
3 comparison to artificial oleosome-like protein-free rapeseed-based emulsion or pure
4 rapeseed oil.

5

6

7

8

9

10

11

12

13

14

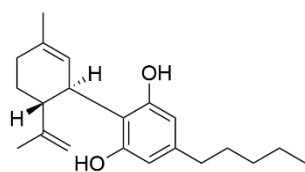
15

16

1 **2. Materials and Methods**

2 **2.1 Materials**

3 Rapeseed oil, sodium hydroxide solution (NaOH, 1 M), potassium bromide (KBr), L-
4 α -phosphatidylcholine (~60%, from egg yolk), Trizma® maleate, sodium taurocholate
5 hydrate, pancreatin from porcine pancreas (8 × USP), 4,4-
6 dichlorodiphenyltrichloroethane (DDT), acetic acid, isooctane, potassium iodide (KI,
7 powder), sodium dodecyl sulphate (SDS), sodium thiosulphate and soluble starch
8 were all purchased from Sigma-Aldrich (Dorset, UK). Synthetic CBD (Fig. 1) was
9 kindly donated by CBDepot.eu (Teplice, Czech Republic). Pooled male Sprague
10 Dawley rat plasma was purchased from Sera Laboratories International Ltd (West
11 Sussex, UK). Rapeseed phosphatidylcholine (PC, > 98%) was purchased from
12 Stratech Scientific (Ely, UK). EnzyChrom™ Triglyceride Assay Kit was purchased
13 from Generon Ltd (Slough, UK). All other solvents were of high-performance liquid
14 chromatography (HPLC) grade or higher.



16 **Figure 1.** 2D structure of cannabidiol (Created by ChemDraw, Revvity Signals
17 Software, Waltham, Ma, US)

18

19 **2.2 Preparation of oleosome-like protein-free artificial emulsion vehicle**

1 The oleosome-like protein-free artificial emulsion preparation procedure was modified
2 from previously reported methodology (Deleu et al., 2010). Rapeseed lecithin (40
3 mg) and rapeseed oil (760 mg) were first added into tubes, followed by addition of
4 1.2 mL water. The mixture was then homogenised using Bandelin Sonopuls HD 2070
5 ultrasonic homogenizer (Berlin, Germany) at 20 kHz, 15 s (full power, 60% cycle,
6 repeated 6 times with 25 s intervals). The emulsion was then cooled on ice for 1 min
7 and filtered using syringe filter (pore size 5 µm). Triglyceride concentrations of the
8 obtained artificial emulsion was measured by EnzyChrom™ triglyceride assay kit
9 using the manufacturer's instructions (BioAssay Systems, Hayward, CA, US).

10

11 **2.3 Preparation of rapeseed oleosomes vehicle**

12 The procedure of extraction of rapeseed oleosomes from rapeseed seeds was based
13 on a previous report (De Chirico et al., 2018). Briefly, rapeseed seeds were soaked in
14 0.1 M sodium bicarbonate buffer (pH 9.5) at 4 °C for 16 hours with a ratio of 1:4
15 (seeds : buffer, w / w). The liquid was then filtered off and seeds were crushed by a
16 Kenwood BLX52 blender (Havant, UK) at full power for 90 s with the same buffer at a
17 ratio of 1:7 (seeds : buffer, w / w). The mixture was filtered and centrifuged at 10000
18 g for 30 minutes at 4 °C using Beckman J2-21 centrifuge, JA-10 rotor (Brea, CA,
19 US). The cream on the upper layer was collected and resuspended by gentle stirring
20 in the sodium bicarbonate buffer 0.1 M (1 : 4, cream : buffer, w : w). Subsequently,
21 the emulsion was centrifuged again (10000 g for 30 minutes at 4 °C). The cream was

1 collected and resuspended in water by gentle stirring (1 : 4, cream : water, w : w).
2 The third centrifugation (10000 g for 30 minutes at 4 °C) was then performed and the
3 cream collected was the final rapeseed oleosomes batch. The triglyceride (TG)
4 concentrations were measured by EnzyChrom™ triglyceride assay kit using the
5 manufacturer's instructions (BioAssay Systems, Hayward, CA, US). The oleosomes
6 were diluted to TG levels of 380 mg/mL with water to resemble TG levels in the
7 artificial emulsion.

8

9 **2.4 Preparation of CBD-loaded artificial emulsion, oleosomes and rapeseed oil**

10 To prepare artificial emulsion loaded with CBD, the drug was pre-dissolved in
11 rapeseed oil at a concentration of 4 mg/mL, and the emulsion was prepared as
12 described above in Section 2.2. For loading CBD into rapeseed oleosomes, 981 µL
13 of rapeseed oleosome emulsion (380 mg/mL TG concentration) were mixed with 19
14 µL solution of 100 mg/mL CBD in ethanol. The mixture was then stirred using a
15 magnetic stirrer (400 RPM) at 37 °C for 1 hour.

16 Density gradient centrifugation (1070 g, 22.5 h) was then applied by Eppendorf®
17 5810R Centrifuge with A-4-62 rotor (Hamburg, Germany) to separate the oleosomes
18 or artificial emulsion from free CBD (Gershkovich and Hoffman, 2005; Muresan et al.,
19 2023; Qin et al., 2021; Zgair et al., 2016). Subsequently, the upper layer containing
20 the cream was collected and diluted in water to reach a TG concentration of 235
21 mg/mL. This resulted in CBD concentration of about 1 mg/mL in drug-loaded

1 oleosomes and artificial emulsion.

2 CBD-loaded rapeseed oil formulation was prepared by solubilising CBD in rapeseed
3 oil at a concentration of 4.44 mg/mL.

4

5 **2.5 Particle size measurement of emulsions**

6 The particle sizes of artificial emulsion and rapeseed oleosomes were measured by
7 HORIBA LA960 laser diffraction particle size distribution analyser (Kyoto, Japan).

8 Emulsion and oleosomes were diluted 5000-fold in water before measurement. All
9 measurements settings were based on previous report (De Chirico et al., 2018).

10 Median particle size and volume distribution were recorded.

11

12 **2.6 Zeta potential measurement of emulsions**

13 A series of 10000-times water-diluted artificial emulsions and rapeseed oleosomes
14 were prepared in 1mL Eppendorf tubes. The pH values were adjusted to be between
15 3 and 10 using 0.1 M NaOH and 0.1 M HCl. Samples were then analysed using
16 Malvern Zetasizer Nano ZS (Malvern, UK). The measurement settings were set
17 based on a previous report (De Chirico et al., 2018).

18

19 **2.7 Triglyceride level determination**

1 Triglycerides levels in artificial emulsion, rapeseed oleosomes and rapeseed oil were
2 tested by colorimetric EnzyChrom™ triglyceride assay kit using the manufacturer's
3 instructions (BioAssay Systems, Hayward, CA, US).

4

5 **2.8 *In vitro* lipolysis**

6 The digestion of CBD-loaded rapeseed oil, rapeseed oleosomes and artificial
7 emulsion was assessed using an *in vitro* lipolysis model, which mimics lipid digestion
8 processes in the small intestine (Benito-Gallo et al., 2015; Benito-Gallo et al., 2016;
9 Feng et al., 2022; Feng et al., 2021a; Feng et al., 2021b; Gershkovich et al., 2012).
10 The complete digestion buffer (pH 6.8) simulating fasted state consisted of 50 mM
11 Trizma® maleate, 150 mM NaCl, 5 mM CaCl₂, 5 mM sodium taurocholate hydrate
12 and 1.25 mM L-α-lecithin. The incomplete digestion buffer (pH 6.8) that was used for
13 lipase preparation consisted of 50 mM Trizma® maleate, 150 mM NaCl and 5 mM
14 CaCl₂. After all components in buffers were solubilised, the pH values of buffers were
15 adjusted to 6.8 at 37 °C. To obtain lipase preparation from porcine pancreatin, 1 g of
16 pancreatin was added into 5 mL incomplete digestion buffer and vortexed for 15 min
17 at room temperature. The supernatant containing the lipase extract was collected
18 after centrifugation at 5 °C, 1794 g for 15 min, and stored on ice. The CBD-loaded
19 artificial emulsion and rapeseed oleosomes (0.9 mL, 1mg/mL CBD concentration), or
20 CBD-loaded rapeseed oil (202.5 µL, 4.44 mg/mL CBD concentration, followed by
21 addition of 697.5 µL water), were premixed with complete digestion buffer (35.5 mL)

1 at 37 °C for 15 min. Then, 3.5 mL of the lipase preparation was added to initiate the
2 lipolysis process and the pH value was maintained at 6.8 by means of Mettler Toledo
3 T50 pH-stat titrator (Greifensee, Switzerland) using 1 M NaOH solution. The
4 termination of reaction was set to the rate of addition of 1 M NaOH dropping below
5 the threshold of 3 µL/min. The lipolysis medium was then separated into three
6 fractions (sediment, micellar and lipid layer) by ultracentrifugation (SORVALL
7 Discovery 100SE ultracentrifuge (Waltham, MA, US), TH-641 rotor, 269071 g, 37 °C,
8 90 min). All fractions were separately collected and stored at -80 °C until analysis for
9 CBD content.

10

11 **2.9 Peroxide value test**

12 Oil contained in CBD-loaded rapeseed oleosomes and the artificial emulsion was
13 released by freezing and thawing (di Bari et al., submitted manuscript). Briefly, the
14 formulations were frozen in -20 °C for 24 hours and then stored at ambient
15 temperature for one hour to allow for complete thawing. The samples were
16 centrifuged at 10000 g for 15 min at ambient temperature using Biosan Microspin 12
17 centrifuge (Riga, Latvia) and released oil in the upper layer was collected.

18 Subsequently, the peroxide values of these released oils and the CBD-loaded
19 rapeseed oil were determined by sodium thiosulfate titration method (The American
20 Oil Chemists' Society, 2011). Oils were weighed (~1 g) and dissolved in 30 mL of the
21 3:2 acetic acid-isooctane mixture. Saturated KI solution (0.5 mL) was added, and the

1 medium was stirred for 1 min. Then, 30 mL of distilled water, 0.5 mL of 10% sodium
2 dodecyl sulphate and 0.5 mL of starch indicator solution were added. The medium
3 was titrated with 0.01M sodium thiosulphate until the disappearance of the blue
4 colour.

5 Peroxide value (milliequivalents peroxide/ 1000 g of oil) was calculated using

6 Equation 1:

$$7 \text{ Peroxide value} = [(V_{oil} - V_{blank}) * M] / m \quad (\text{Eq. 1})$$

8 where V_{oil} is the titration volume of oil in mL, V_{blank} is the titration volume of blank in
9 mL, M is the molarity of sodium thiosulphate solution in mmol/mL and m is the mass
10 of oil in kg.

11

12 **2.10 *In vivo* pharmacokinetics and biodistribution**

13 All experimental protocols were authorised by the United Kingdom Home Office and
14 University of Nottingham Ethical Review Committee in accordance with the Animals
15 [Scientific procedures] Act 1986. *In vivo* pharmacokinetics and biodistribution studies
16 were carried out using male Sprague Dawley rats, 276 to 300 g body weight (Charles
17 River UK, Margate, UK). The animals were kept in the University of Nottingham Bio-
18 Support Unit (BSU) under regulated temperature and humidity, 12 h light-dark cycle.

19 In the pharmacokinetic study, the right jugular vein was cannulated under general

1 anaesthesia and rats were allowed two nights of recovery. Animals were fasted
2 overnight for up to 16 hours before pharmacokinetic study with free access to water.
3 Three lipid-based formulations of CBD: CBD-loaded rapeseed oil, artificial emulsion
4 and rapeseed oleosomes were administered by oral gavage to animals. Water was
5 administered by a second oral gavage in CBD-loaded rapeseed oil group to provide
6 the same volume of water that is contained in CBD-loaded artificial emulsion and
7 rapeseed oleosomes. The dose of CBD was 3 mg/kg in all groups. CBD-loaded
8 rapeseed oleosomes and artificial emulsion contained 1 mg/mL CBD. CBD-loaded
9 rapeseed oil contained 4.44 mg/mL of CBD and was administered to rats with water
10 at a ratio of 22.5 : 77.5 (oil / water, v / v) to achieve the same dose of CBD, oil and
11 water across all formulations. During pharmacokinetic study, 0.3 mL blood samples
12 were collected from jugular vein cannula at 1, 2, 3, 4, 5, 6, 8, 10 and 12 hours
13 following oral administration into EDTA-containing tubes. Collected blood samples
14 were centrifuged at 3000 g for 10 mins at 4 °C using DLAB D1524R centrifuge
15 (Beijing, China) for plasma separation. All samples were stored at -80 °C until
16 analysis.

17 For biodistribution studies, the rats were fasted up to 16 h with free access to water.
18 The same formulations and doses of CBD were administered by oral gavage to rats.
19 Blood was collected under terminal anaesthesia from inferior vena cava at the
20 plasma t_{max} and $t_{max} - 1$ h (determined in pharmacokinetic studies). Rats were then
21 sacrificed, and lymph fluid sample, mesenteric lymph nodes (MLN), brain, as well as
22 spinal cord tissues were harvested. Collected blood samples were centrifuged at

1 3000 g for 10 mins at 4 °C using DLAB D1524R centrifuge (Beijing, China) to
2 separate plasma. Plasma, lymph, and tissues samples were stored at -80 °C until
3 analysis (Zgair et al., 2017; Zgair et al., 2015).

4

5 **2.11 Bioanalytical Conditions**

6 The concentrations of CBD in all samples were analysed using a HPLC system
7 consisting of Waters Alliance 2695 separations module (Milford, MA, US) and Waters
8 photodiode array ultraviolet (PDA) 2996 detector (Milford, MA, US). The samples
9 preparation procedure and chromatography conditions for determination of CBD
10 were identical to a previously reported methodology (Feng et al., 2022; Feng et al.,
11 2021a; Feng et al., 2021b; Zgair et al., 2015).

12

13 **2.12 Data analysis**

14 All data are presented as mean \pm standard deviation (SD). Phoenix WinNonlin 6.3
15 Professional (Pharsight, Mountain View, CA, US) was used for non-compartmental
16 analysis of plasma concentration-time profiles to obtain pharmacokinetic parameters.
17 Power calculations (G*Power 3.1, Heinrich-Heine-Universität Düsseldorf, Düsseldorf,
18 Germany) were used to determine the sample size of each group (Faul et al., 2007).
19 GraphPad Prism 10.1.0 (GraphPad software, San Diego, CA, US) was used to
20 perform statistical analysis. One-way analysis of variance (ANOVA), followed by

1 Tukey's post-hoc comparison or unpaired t test where appropriate were used for
2 analysis of differences between means. $P < 0.05$ was considered statistically
3 significantly different.

4

5

6

7

8

9

10

11

12

13

14

15

16

1 **3. Results**

2 **3.1 Physicochemical properties of CBD-loaded rapeseed oleosomes and**
3 **artificial emulsion**

4 An artificial emulsion was designed to have similar physicochemical properties as
5 rapeseed oleosomes, including particle size of around 1 μm (Fig. 2A & 2C, Table 1).

6 After CBD-loaded rapeseed oleosomes and artificial emulsion were prepared,

7 various parameters were tested to ensure that they remain similar in their

8 physicochemical characteristics. The particle volume distribution of CBD-loaded

9 rapeseed oleosomes and artificial emulsion is presented in Fig. 2B showing

10 overlapping particle size distributions. However, both CBD-loaded rapeseed

11 oleosomes and artificial emulsion had a higher median particle size (around 2 μm)

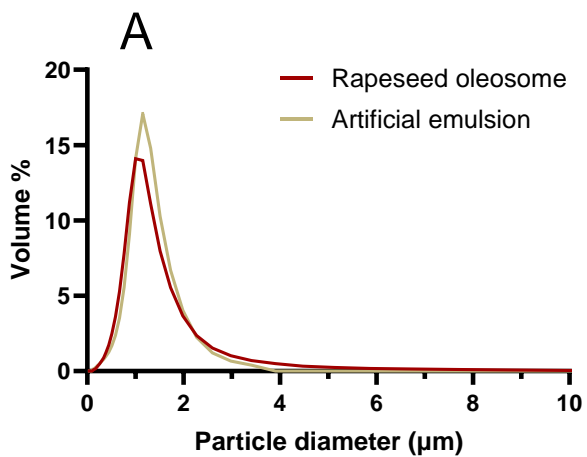
12 compared with unloaded lipid vehicles (Fig. 2B and Table 1). Zeta potential of these

13 two formulations was also similar (Fig. 2D). In addition, Table 1 also shows that CBD-

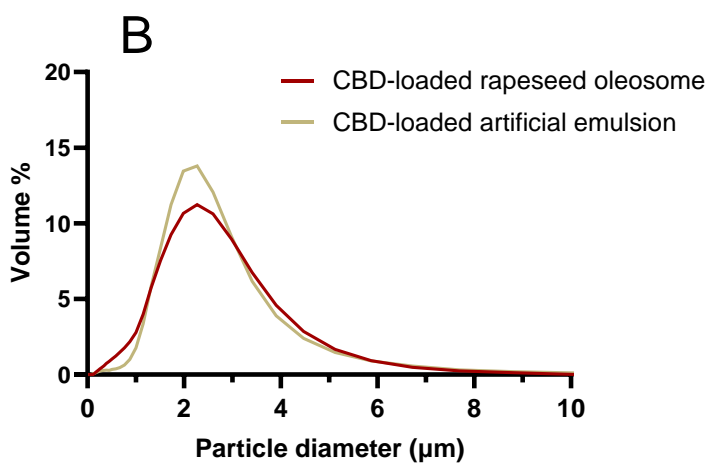
14 loaded rapeseed oleosomes and CBD-loaded artificial emulsion had practically

15 identical CBD concentrations, while triglycerides content was already adjusted to be

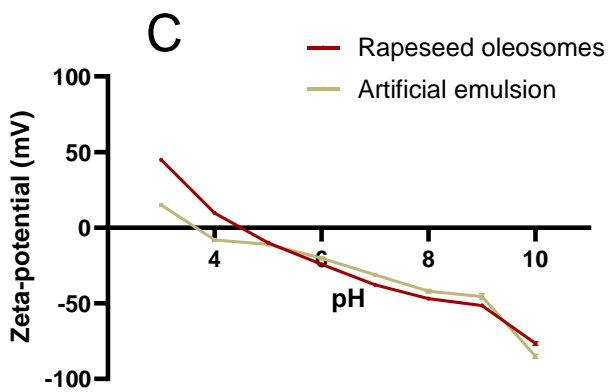
16 equivalent between these two formulations.



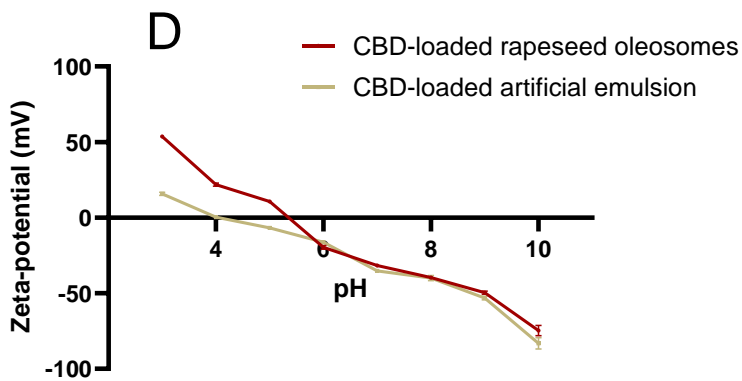
1



2



3



4

1 **Figure 2.** Particle volume distribution and zeta-potential of rapeseed oleosomes and
 2 artificial emulsion before and after CBD loading (n=3). A, volume distribution of
 3 rapeseed oleosomes and artificial emulsion; B, volume distribution of CBD-loaded
 4 rapeseed oleosomes and artificial emulsion; C, Zeta-potential of rapeseed
 5 oleosomes and artificial emulsion; D, Zeta-potential of CBD-loaded rapeseed
 6 oleosomes and artificial emulsion. Unpaired t test was used for analysis of
 7 differences in zeta potential values between artificial emulsion and rapeseed
 8 oleosomes at the same pH with or without CBD. It was found that almost all zeta
 9 potential values of artificial emulsion have significant differences compared with
 10 rapeseed oleosomes, except CBD-loaded artificial emulsion and CBD-loaded
 11 rapeseed oleosomes at pH 8. P < 0.05 was considered statistically significantly
 12 different.

13

14 **Table 1**

15 Properties of CBD-loaded rapeseed oleosomes and artificial emulsion (Mean \pm SD,
 16 n=3)

	TG level (mg/mL*)	Median particle size (μm)	CBD concentration (mg/mL)
Artificial emulsion	382.57 \pm 24.50	1.09 \pm 0.01 ^{ns}	-
Rapeseed oleosomes	Adjusted to be identical to artificial emulsion	1.00 \pm 0.06	-
CBD-loaded artificial emulsion	235.36 \pm 11.44	2.03 \pm 0.15 ^{ns}	1.04 \pm 0.03 ^{ns}
CBD-loaded rapeseed oleosomes	Adjusted to be identical to CBD-loaded artificial emulsion	1.94 \pm 0.04	1.03 \pm 0.07

17 *Triglyceride levels are expressed as mg/mL triolein equivalents. The unit conversion
 18 formula is as follows:

19 1.0 mmol/L triglycerides = 0.885 mg/mL triolein equivalent triglycerides.

20 The measured triglycerides concentration of pure rapeseed oil was 1043 \pm 81
 21 mg/mL.

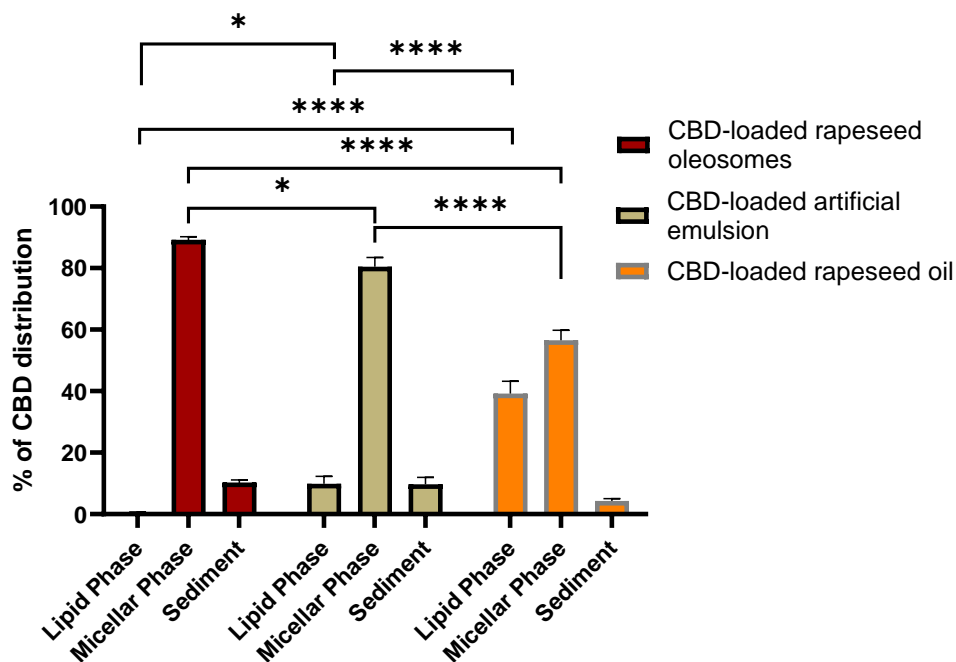
22 ^{ns} not significantly different from corresponding oleosomes groups. Statistical analysis

1 was performed using unpaired t test between artificial emulsion and rapeseed
2 oleosomes groups with or without CBD. P < 0.05 was considered to represent a
3 significant difference.

4

5 **3.2 *In vitro* lipolysis of CBD-loaded rapeseed oil, rapeseed oleosomes and** 6 **artificial emulsion**

7 The distribution of CBD into the sediment, aqueous micellar and oil phases following
8 *in vitro* lipolysis of CBD-loaded rapeseed oil, rapeseed oleosomes and artificial
9 emulsion is shown in Fig. 3. The drug recovered in aqueous micellar phase is
10 considered to be readily available for absorption. The CBD distributed more
11 efficiently into micellar phase following lipolysis of CBD-loaded rapeseed oleosomes
12 than following lipolysis of other formulations. The sodium hydroxide solution volumes
13 used for titration during the lipolysis of three formulations were 0.49 ± 0.02 mL, 0.26
14 ± 0.04 mL and 0.12 ± 0.00 mL (mean \pm SD, rapeseed oleosome, artificial emulsion,
15 rapeseed oil, respectively).



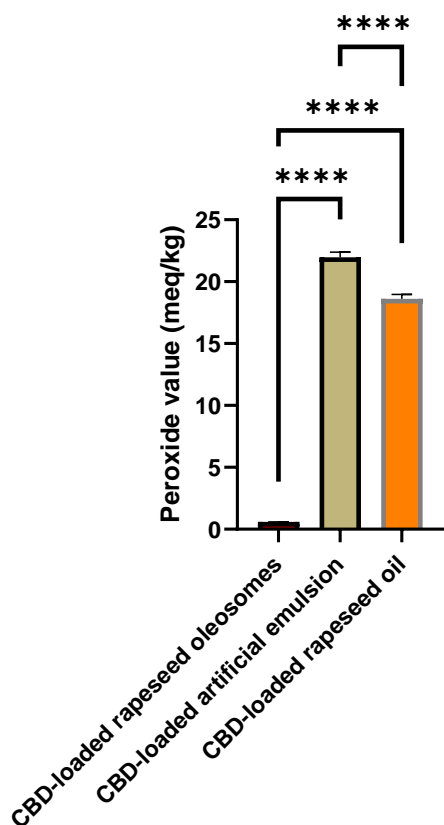
1

2 **Figure 3.** CBD partitioning into lipid, micellar aqueous, and sediment phases after *in*
 3 *vitro* lipolysis of CBD-loaded rapeseed oil, rapeseed oleosomes and artificial
 4 emulsion. (mean ± SD, n = 3). One-way ANOVA, followed by Tukey’s multiple
 5 comparisons test was applied to evaluate the statistical significance of differences
 6 between means of CBD distribution into three phases. *, p < 0.05, ****, p < 0.0001.

7

8 **3.3 Peroxide value of CBD-loaded rapeseed oil and released oils from CBD-**
 9 **loaded rapeseed oleosomes and artificial emulsion**

10 The peroxide values of released oil from CBD-loaded rapeseed oleosomes and
 11 artificial emulsion, as well as of CBD-loaded rapeseed oil formulation were assessed
 12 (Fig. 4). The oil released from rapeseed oleosomes had a dramatically lower
 13 peroxide value than of other formulations.



1

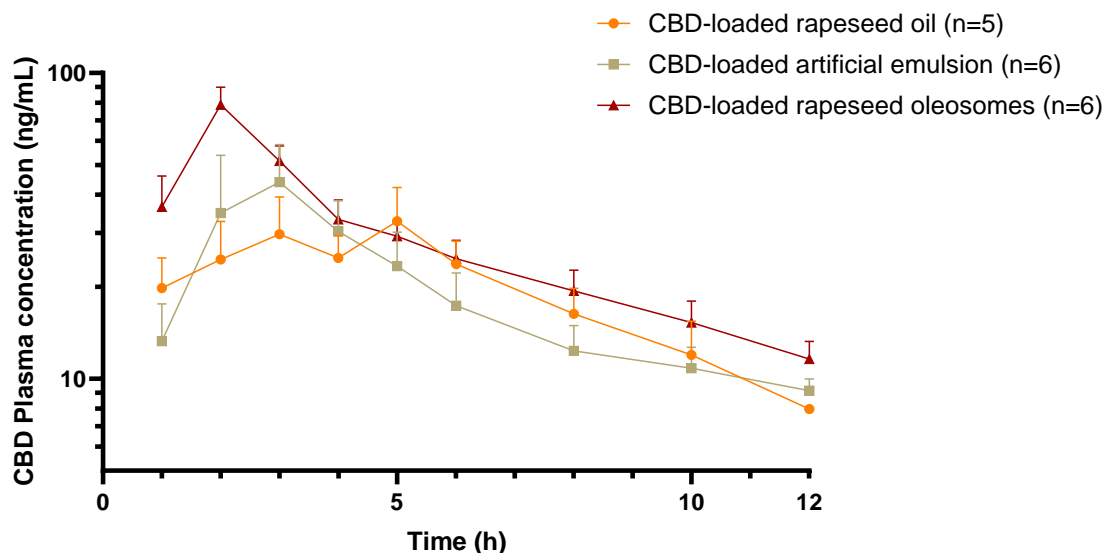
2 **Figure 4.** Peroxide value for different rapeseed-based formulations (Mean \pm SD,
3 $n=3$). ****, $P < 0.0001$. One-way ANOVA, followed by Tukey 's multiple comparisons
4 test was applied to evaluate the statistical significance of differences between
5 means.

6

7 **3.4 Pharmacokinetics of CBD following oral administration in different** 8 **formulations**

9 The plasma concentration-time profiles of CBD following oral gavage administration
10 of CBD-loaded rapeseed oil, artificial emulsion and rapeseed oleosomes are shown
11 in **Fig. 5**. The pharmacokinetic parameters derived from plasma concentration-time
12 profiles are shown in Table 2. The CBD-loaded rapeseed oleosomes led to the
13 highest systemic exposure to CBD (AUC) and highest C_{max} in comparison to other
14 formulations (2-fold increase versus rapeseed oil). C_{max} was also reached faster with

1 CBD-loaded rapeseed oleosomes ($t_{max} = 2$ h) than that of CBD-loaded rapeseed oil
 2 ($t_{max} = 5$ h) and artificial emulsion ($t_{max} = 2-3$ h).



3

4 **Figure 5.** Plasma CBD concentrations-time profile following oral administration of 3
 5 mg/kg CBD in different formulations in Sprague Dawley rats (Mean \pm SD, n = 5/6).

6

7 **Table 2**

8 Plasma pharmacokinetic (PK) parameters of CBD following oral administration of
 9 CBD in different formulations (Mean \pm SD).

Formulations	$t_{1/2}$ ^a (h)	t_{max} ^b (h)	C_{max} ^c (ng/mL)	AUC _{0-∞} ^d (h × ng/mL)	F ^e (%)	n
CBD-loaded rapeseed oil	3.5 \pm 0.4	5	36 \pm 8	273 \pm 58	17.6 \pm 3.8	5
CBD-loaded artificial emulsion	3.6 \pm 0.8	2-3	50 \pm 13	258 \pm 53	16.7 \pm 3.4	6
CBD-loaded rapeseed oleosomes	4.0 \pm 0.7	2	79 \pm 11	413 \pm 25 ^{***}	26.7 \pm 1.6 ^{***}	6

10 ^a half-life; ^b time to maximum concentration in plasma; ^c the maximum concentration
 11 in plasma; ^d area under the curve (AUC) from 0 to infinity; ^e bioavailability calculated
 12 based on (Zgair et al., 2015).

13 ^{***}, statistically significantly different from rapeseed oil and artificial emulsion groups
 14 (P < 0.001, one-way ANOVA followed by Tukey's multiple comparisons test within 3
 15 lipid-based formulations).

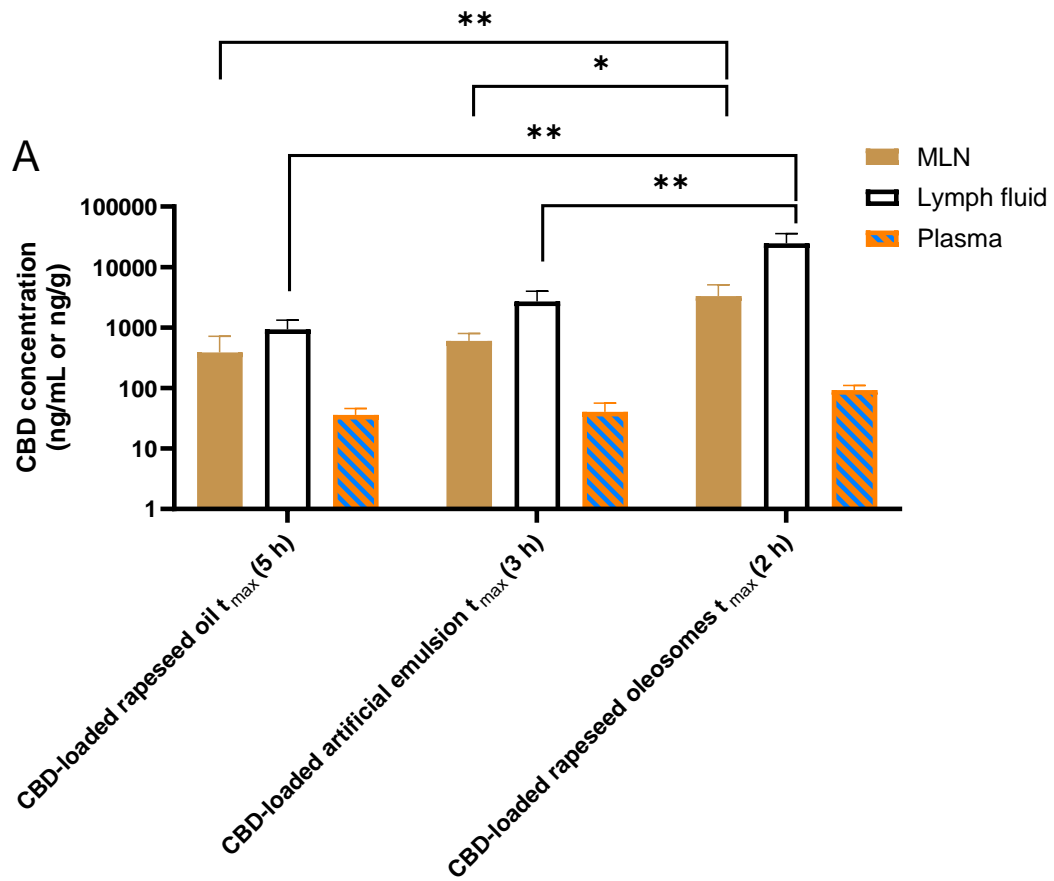
1

2 **3.5 Biodistribution of CBD following oral administration**

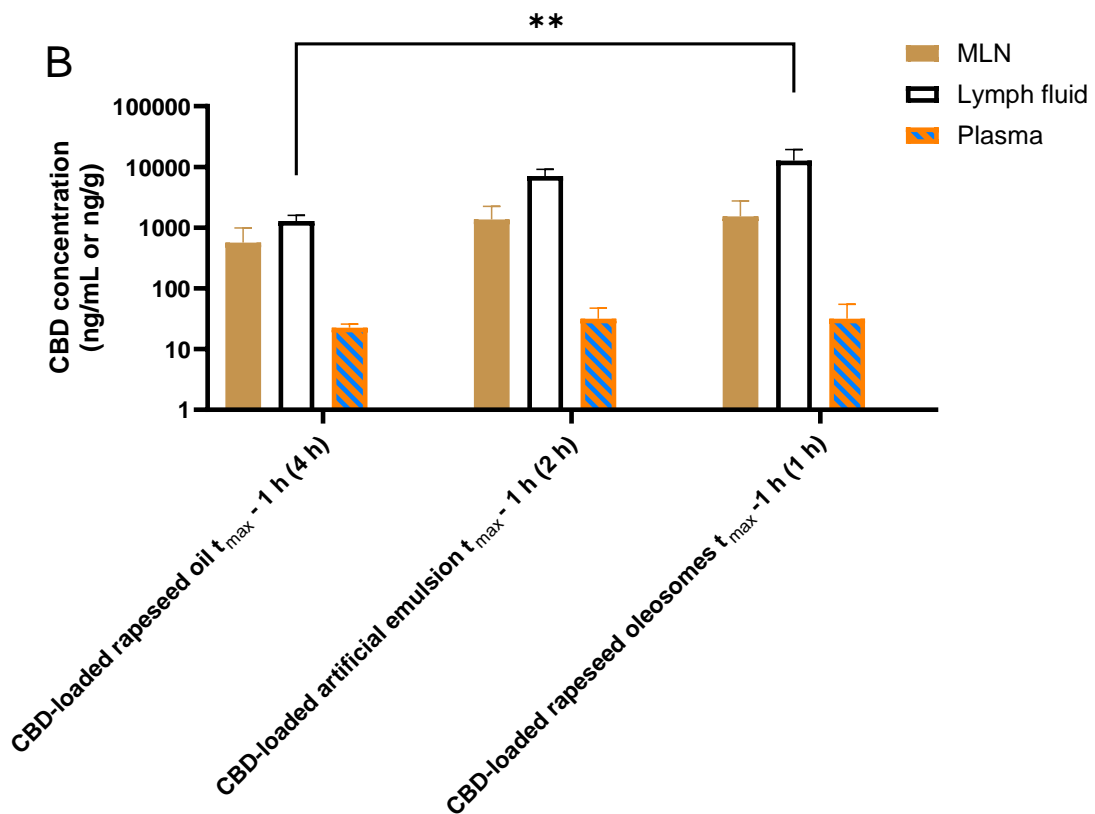
3 Plasma, lymph fluid, mesenteric lymph nodes (MLN), brain and spinal cord were
4 obtained at plasma t_{max} and $t_{max} - 1$ h following oral administration of CBD-loaded
5 rapeseed oil, artificial emulsion and rapeseed oleosomes. The results are shown in
6 **Fig. 6A and 6B**. At plasma t_{max} , the CBD-loaded rapeseed oleosomes led to a
7 significantly higher CBD concentration in MLN and lymph fluid compared with the
8 CBD-loaded artificial emulsion and rapeseed oil (**Fig. 6A**). At t_{max} , the concentration of
9 CBD in MLN following administration of CBD-loaded rapeseed oleosomes was 8.5-
10 fold and 5.5-fold higher than following administration of CBD-loaded rapeseed oil or
11 CBD-loaded artificial emulsion, respectively. In lymph fluid, CBD-loaded rapeseed
12 oleosomes led to 26.5-fold and 9.2-fold higher CBD concentration than following
13 CBD-loaded rapeseed oil and artificial emulsion administrations, respectively. At $t_{max} -$
14 1 h, the concentrations of CBD in MLN and lymph fluid following oral administration
15 of CBD-loaded rapeseed oleosomes were also higher than for other groups (**Fig. 6B**).
16 However, the differences at $t_{max} - 1$ h were less prominent than for plasma t_{max} . The
17 distribution of CBD was also assessed in brain and spinal cord tissues and described
18 in Supplementary Material Fig. S1.

19

[Type here]



1



2

1 **Figure 6.** Biodistribution of CBD at plasma t_{max} and $t_{max} - 1h$ following oral
2 administration of 3 mg/kg CBD in different formulations in Sprague Dawley rats
3 (Mean \pm SD, n = 4). MLN, mesenteric lymph nodes. A, biodistribution of CBD at
4 plasma t_{max} ; B, biodistribution of CBD at plasma $t_{max} - 1h$. One-way ANOVA, followed
5 by Tukey 's multiple comparisons test was applied to evaluate the statistical
6 significance of differences between means. *, p < 0.05, **, p < 0.01.

7

8

9

10

11

12 **4. Discussion**

13 Lipid-based formulations are an effective strategy to increase the intestinal lymphatic
14 delivery and oral bioavailability of highly lipophilic drugs (Feeney et al., 2016; Hauss,
15 2007; Porter et al., 2007). On the example of a highly lipophilic drug CBD, we have
16 previously shown that natural vegetable oil vehicles led to higher intestinal lymphatic
17 delivery and systemic bioavailability than pre-digested or self-emulsifying drug
18 delivery systems (Feng et al., 2021a; Feng et al., 2021b). However, even the best
19 performing vegetable oil vehicles (sesame and olive oils) resulted in systemic
20 bioavailability of CBD of only about 20% (Feng et al., 2022; Zgair et al., 2016).

21 Therefore, inspired by the superior performance of natural vegetable oils in

22 comparison to artificial formulations *in vivo* (Feng et al., 2021a; Feng et al., 2021b), in

1 this work we have assessed the natural seed-derived oleosomes as an oral
2 formulation vehicle for CBD. Oleosomes are triglyceride-rich particles surrounded by
3 phospholipid monolayer with embedded proteins, the so called oleosins. The
4 performance of CBD-loaded rapeseed oleosomes as a formulation for lymphatic
5 delivery and systemic bioavailability following oral administration was compared with
6 CBD-loaded rapeseed oil and rapeseed artificial emulsion controls.

7

8 **4.1 The physicochemical properties of CBD-loaded rapeseed oleosomes and** 9 **artificial emulsion**

10 After drug loading and density gradient centrifugation (to remove free CBD), around 1
11 mg/mL CBD content was found in the CBD-loaded oleosomes with a triglyceride
12 concentration of approximately 235 mg/mL (Table 1). To assess the possible
13 influence of various characteristics of rapeseed oleosomes on the absorption and
14 lymphatic delivery of CBD, a protein-free CBD-loaded artificial emulsion was
15 developed. The CBD-loaded artificial emulsion was designed to be similar to CBD-
16 loaded rapeseed oleosomes in terms of rapeseed oil as a lipid core, rapeseed
17 phospholipids as surface active agents, median particle size, triglyceride levels, and
18 CBD content (Fig. 2B, Table 1). These two formulations also showed overall similar
19 values for their zeta-potential (Fig. 2D). However, since there is no protein in the
20 artificial emulsions, zeta potential of the CBD-loaded artificial emulsion was slightly
21 different from CBD-loaded rapeseed oleosomes in the pH range. Considering the

1 acidic pH environment of gastrointestinal tract (Fallingborg, 1999; McConnell et al.,
2 2008), this difference may slightly affect formulations' behaviour in the stomach.
3 Additionally, another noteworthy phenomenon is the change in particle size and zeta
4 potential before and after CBD loading. Before CBD loading, both artificial emulsion
5 and rapeseed oleosomes had a median particle size of approximately 1 μm (Fig. 2A,
6 Table 1). After CBD loading, their median particle size increased to around 2 μm (Fig.
7 2B, Table 1). Although the drug loading could be responsible for this increase the
8 particle size, the main reason is most likely due to density gradient centrifugation,
9 which is used to separate the formulation from the unloaded free CBD (see
10 Supplementary Material Fig. S2). Despite particle size increase, these two
11 formulations showed only slight changes in zeta potential before and after CBD
12 loading (Fig. 2C & 2D).

13

14 **4.2 CBD-loaded rapeseed oleosomes improves the intestinal lymphatic delivery** 15 **and systemic bioavailability of CBD compared with CBD-loaded rapeseed oil** 16 **and rapeseed artificial emulsion**

17 Oil-in-water emulsions can enhance the oral bioavailability of lipophilic drugs
18 (McClements, 2018). However, in this work, the artificial emulsion enhanced the
19 absorption rate and plasma C_{max} in comparison to CBD-loaded pure rapeseed oil, but
20 did not change the AUC, which represents the overall systemic exposure to the drug
21 and its bioavailability (Fig. 5, Table 2). The CBD-loaded artificial emulsion also
22 increased the lymphatic delivery of CBD at plasma t_{max} and $t_{\text{max}} - 1$ h compared with

1 rapeseed oil (Fig. 6A & 6B). Nevertheless, in comparison to rapeseed oleosomes,
2 this improvement is not significant. The enhanced CBD absorption rate, plasma C_{max}
3 and lymphatic delivery of CBD at plasma t_{max} and $t_{max} - 1$ h by artificial emulsion
4 compared with rapeseed oil could be explained by the difference in their composition.
5 The CBD-loaded rapeseed oil formulation consists only of CBD solubilised in pure oil
6 and is not pre-emulsified. Therefore, it is likely to be digested and absorbed at a
7 slower rate relative to the pre-emulsified formulations, which is indeed supported by
8 the results of this study (Fig. 5). Moreover, *in vitro* lipolysis of the CBD-loaded
9 rapeseed oil resulted in a substantially higher distribution of CBD into the undigested
10 oil fraction compared with the other formulations (Fig. 3), further supporting the *in*
11 *vivo* findings of slower absorption of CBD following administration of this formulation
12 in comparison to pre-emulsified vehicles.

13 On the other hand, oral administration of CBD-loaded rapeseed oleosomes resulted
14 in the fastest CBD absorption and highest plasma C_{max} , as well as substantially
15 higher bioavailability in comparison to the other two lipid-based formulations.

16 Importantly, CBD-loaded rapeseed oleosomes achieved significantly higher lymphatic
17 delivery of CBD in comparison to CBD-loaded rapeseed oil or artificial emulsion (Fig.
18 6A & 6B). One possible explanation for the superior performance of the CBD-loaded
19 oleosomes in comparison with the CBD-loaded artificial emulsion could be decreased
20 coalescence of oleosomes during the early stages of digestion. As mentioned in
21 Section 4.1, zeta potential of CBD-loaded artificial emulsion under acidic environment
22 was lower than that of CBD-loaded rapeseed oleosomes (Fig. 2D). Since a lower

1 absolute zeta potential value normally represent the lower stability of emulsion
2 (Bhattacharjee, 2016; Kaszuba et al., 2010), this may lead to enhanced coalescence
3 of the CBD-loaded artificial emulsion in the stomach. In addition, the presence of
4 proteins on the surface of oleosomes could lead to lower coalescence (De Chirico et
5 al., 2018; Deleu et al., 2010; Nikiforidis, 2019; Tzen and Huang, 1992; White et al.,
6 2009). Thus, the eventual size of oleosomes' droplets within the intestinal tract *in vivo*
7 might be smaller than that of the artificial emulsion and this could favour the lipolysis
8 process by digestive lipases (Benzonana and Desnuelle, 1965). The
9 physicochemical properties of lipid droplets appearing in the intestinal lumen can
10 significantly affect the rate of lipid digestion and affect the bioavailability of loaded
11 drugs (McClements, 2018; Salvia-Trujillo et al., 2013b; Salvia-Trujillo et al., 2017).
12 Smaller droplet size of the emulsion droplets often leads to faster and more complete
13 lipid digestion, efficient formation of mixed micelles, and eventually higher
14 bioavailability of formulated drugs (Salvia-Trujillo et al., 2013b, a; Yi et al., 2014).
15 Therefore, although the particle size of the CBD-loaded artificial emulsion was
16 designed to be similar to the particle size of CBD-loaded oleosomes before
17 administration, oleosome formulation could lead to smaller size of droplets within the
18 gastrointestinal tract, eventually resulting in higher bioavailability and intestinal
19 lymphatic delivery of CBD. However, there is currently a lack of direct evidence
20 regarding the changes in particle size of these two formulations during digestion to
21 support this hypothesis.

22 Another potential explanation of the differences in oral bioavailability and lymphatic

1 delivery of CBD between CBD-loaded oleosomes and artificial emulsion is that the
2 proteins on the surface of oleosomes could influence the intraluminal digestion or
3 affect various stages of intra-cellular assembly and release of chylomicrons. The
4 proteins present on the oleosome membrane are mainly oleosins (15 - 20 kDa), in
5 addition to caleosins (25 - 35 kDa), and steroleosins (> 35 kDa) (Nikiforidis, 2019).
6 The structures of these proteins have certain similarities with surfactants - the
7 hydrophobic domains are anchored in the triacylglycerol core, while the hydrophilic
8 domains are exposed to the aqueous phase (Jolivet et al., 2017; Nikiforidis, 2019).
9 Some previous studies have demonstrated that the presence and type of proteins
10 can affect the lipolysis of emulsions *in vitro* (Beisson et al., 2001; Ding et al., 2021;
11 Ding et al., 2020). In addition, Couëdelo reported that the type of emulsifier could
12 affect the expression of genes that are involved in absorption of fatty acids and
13 chylomicron assembly and secretion in rats (Couëdelo et al., 2015). These results
14 indicate the potential role of proteins in oleosomes on the absorption of CBD.

15 An *in vitro* model of lipid digestion was used to explore what might be occurring
16 during the digestion of CBD-loaded lipid droplets in rats (Fig. 3). During lipolysis,
17 substantially higher amount of sodium hydroxide solution was consumed during the
18 digestion of the CBD-loaded rapeseed oleosomes in comparison with the CBD-
19 loaded artificial emulsion and CBD-loaded rapeseed oil (0.49 mL, 0.26 mL and 0.12
20 mL, respectively). This leads to an estimated hydrolysis levels of these three
21 formulations of $68.34 \pm 2.79\%$, $36.21 \pm 5.57\%$ and $16.76 \pm 0.56\%$ (mean \pm SD, CBD-
22 loaded rapeseed oleosomes, artificial emulsion and rapeseed oil, respectively). This

1 means that the CBD-loaded oleosomes were hydrolysed most efficiently in
2 comparison with the artificial emulsion and rapeseed oil systems. The hydrolysis
3 level reached with rapeseed oleosomes corresponds to the release of two fatty acids
4 out of the three esterified in rapeseed triglycerides, i.e. the complete conversion of
5 triglycerides into free fatty acids and monoglycerides. This suggests that the lipids
6 initially present in the oleosomes could be all transferred to the micellar phase where
7 they can contribute to the formation of mixed micelles with bile salts and
8 phospholipids. The process could increase the micellar solubilization of CBD and,
9 indeed, the highest level of CBD in the micellar phase is observed with CBD-loaded
10 oleosomes (Fig. 3). However, on this important parameter - the CBD distribution
11 fraction, the performance of CBD-loaded rapeseed oleosomes did not differ
12 significantly from CBD-loaded artificial emulsion. The lipolysis of the CBD-loaded
13 oleosomes led to ~90% of CBD distribution into micellar phase and very little CBD
14 was left for the undigested oil phase (very little volume of oil left). For artificial
15 emulsion, the CBD distribution into micellar phase and oil phase was ~80% and
16 ~10%, respectively. Moreover, this *in vitro* lipolysis model only simulates the pre-
17 enterocyte intestinal digestion processes. Since CBD is a highly lipophilic molecule,
18 its oral bioavailability is greatly affected by the intestinal lymphatic transport, which is
19 associated with affinity to chylomicrons in the enterocytes. It has been suggested
20 previously that *in vitro* lipolysis models might be not predictive for oral bioavailability
21 of drugs with substantial intestinal lymphatic transport component in their absorption
22 following oral administration (Chu et al., 2023; Dahan and Hoffman, 2008). These

1 considerations suggest that differences in intraluminal digestion of these two
2 formulations could partially contribute to the differences in oral bioavailability and
3 lymphatic delivery of CBD. It is, however, unlikely, that the observed differences in
4 CBD distribution into micellar, oil and sediment phases following the *in vitro* lipolysis
5 can fully explain the substantially higher lymphatic delivery and bioavailability of CBD
6 following oral administration of CBD-loaded oleosomes *in vivo*. In addition, there is
7 still insufficient evidence to explain how the hydrolysis rate of triglycerides could
8 make an impact on the distribution of CBD.

9 Another hypothesis is that the oxidation level of lipids in the formulation could affect
10 the oral bioavailability and lymphatic delivery of CBD. Polyunsaturated oils are prone
11 to formation of peroxides during processing and storage and could potentially also
12 undergo oxidation in the gastrointestinal tract following administration (Nieva-
13 Echevarría et al., 2020). The initial oxidation of lipids may lead to reduced lipolysis
14 (Martin-Rubio et al., 2019). This could explain at least partially the sodium hydroxide
15 titration volume differences during lipolysis. On the other side, the oxidation level of
16 lipids could substantially affect the digestion and absorption of lipids and the
17 bioavailability of lipophilic drugs (Márquez-Ruiz et al., 2008; Yao et al., 2022). It was
18 reported that the quantity and morphology of lipoprotein particles produced by
19 intestinal epithelial cells depends on the oxidation state of the administered lipids,
20 with oxidized lipids leading to smaller and more irregularly shaped lipoproteins (Yao
21 et al., 2022). In addition, exposure to oxidized lipids might adversely affect the
22 intestinal epithelial cells and subsequently influence the absorption of lipophilic

1 substances (Yao et al., 2022). Furthermore, the oxidation of oil could also affect the
2 minor constituents present in the natural oils, such as sterols and phenolic
3 compounds (Márquez-Ruiz et al., 2008). The presence of these minor constituents
4 could be one of the factors responsible for higher oral bioavailability and lymphatic
5 delivery of CBD observed with natural vegetables oils in comparison to pre-digested
6 or other artificial formulations (Feng et al., 2021a). To test this hypothesis, the lipids
7 in the three formulations were extracted and the peroxide value was assessed (Fig.
8 4). The results show that the oil from CBD-loaded rapeseed oleosomes has
9 dramatically lower peroxide value (~0.6 meq/kg) than that from the CBD-loaded
10 artificial emulsion (~22.0 meq/kg). The peroxide value of CBD-loaded rapeseed oil is
11 close to the oil from CBD-loaded artificial emulsion (~18.6 meq/kg). Given the
12 dramatic difference in the peroxide values of the oil content of the CBD-loaded
13 rapeseed oil, artificial emulsion and oleosomes, degree of oxidation of lipids could be
14 an important factor for the differences observed in the lymphatic delivery and
15 bioavailability of CBD. Further research will be needed to confirm or reject this
16 hypothesis, as well as for mechanistic investigation of how the degree of oxidation
17 affects the digestion of lipids, the bioavailability and lymphatic delivery of lipophilic
18 drugs.

19

20

21

1

2

3

4

5

6

7

8 **5. Conclusion**

9 CBD has low oral bioavailability due to its high lipophilicity and extensive first-pass
10 metabolic loss. Lipid-based formulations containing long-chain triglyceride or long-
11 chain fatty acids are an effective strategy to facilitate the intestinal lymphatic delivery
12 and enhance oral bioavailability of this lipophilic drug. Our previous work suggests
13 that natural vegetable oils lead to higher lymphatic delivery and systemic
14 bioavailability of CBD in comparison to pre-digested or self-emulsifying artificial
15 formulations. In this work, we have developed a novel formulation of CBD based on
16 natural rapeseed oleosomes and compared its CBD delivery performance to pure
17 rapeseed oil and artificial oleosome-like rapeseed-based emulsion. The CBD-loaded
18 rapeseed oleosomes led to substantially higher lymphatic delivery and systemic
19 bioavailability of CBD in comparison with artificial rapeseed oil emulsion (stabilised

1 with rapeseed phosphatidylcholine) or non-emulsified rapeseed oil. The lower
2 oxidation level of the oil in oleosomes could be an important factor for the observed
3 superior performance of natural oleosomes. Other potential explanations could
4 include differences in intraluminal stability post-administration, influence of the
5 surface proteins during the intraluminal digestion or the assembly and release of
6 chylomicrons, or the lipolysis efficiency of the lipid vehicles. Further investigation is
7 necessary to confirm or reject these hypotheses, as well as for mechanistic
8 investigation on how the degree of oxidation, the presence of protein and other
9 factors affect the digestion of lipids, the bioavailability and lymphatic delivery of CBD
10 and other lipophilic drugs.

11

12 **CRedit authorship contribution statement**

13 **Liuhan Ji**: Conceptualization, Investigation, Methodology, Data curation, Writing -
14 review & editing, Writing - original draft. **Wanshan Feng**: Investigation. **Haojie Chen**:
15 Investigation. **YenJu Chu**: Investigation. **Abigail Wong**: Investigation. **Yufei Zhu**:
16 Investigation. **Graziamarina Sinatra**: Investigation. **Filippo Bramante**: Investigation.
17 **Frederic Carriere**: Writing - review & editing. **Michael Stocks**: Supervision.
18 **Vincenzo Di Bari**: Writing - review & editing. **David Gray**: Supervision, Writing -
19 review & editing. **Pavel Gershkovich**: Conceptualization, Methodology, Supervision,
20 Resources, Project administration, Writing - review & editing.

1

2

3 **Acknowledgements**

4 The authors would like to acknowledge the CBDepot.eu for their kindly donation of
5 synthetic CBD. The authors also would like to thank the Bio-Support Unit (BSU) team
6 in the University of Nottingham for excellent technical assistance.

7

8 **Funding sources**

9 This work was supported by Rosetrees Trust and Stoneygate Trust [grant number
10 M902].

11 **References**

- 12 Alice Brookes, N.K., David J. Scurr, Morgan R. Alexander, Pavel Gershkovich, Tracey
13 D. Bradshaw, 2024. Cannabidiol and fluorinated derivative anti-cancer properties
14 against glioblastoma multiforme cell lines, and synergy with imidazotetrazine agents.
15 BJC Reports. <https://doi.org/10.21203/rs.3.rs-3639079/v1>.
- 16 Arzimanoglou, A., Brandl, U., Cross, J.H., Gil-Nagel, A., Lagae, L., Landmark, C.J.,
17 Specchio, N., Nabbout, R., Thiele, E.A., Gubbay, O., Panel, a.o.m.o.T.C.I.E., 2020.
18 Epilepsy and cannabidiol: a guide to treatment. *Epileptic Disorders* 22, 1-14.
19 <https://doi.org/10.1684/epd.2020.1141>.
- 20 Beisson, F., Ferté, N., Bruley, S., Voultoury, R., Verger, R., Arondel, V., 2001. Oil-bodies
21 as substrates for lipolytic enzymes. *Biochimica et Biophysica Acta (BBA)-Molecular
22 and Cell Biology of Lipids* 1531, 47-58. [https://doi.org/10.1016/S1388-
23 1981\(01\)00086-5](https://doi.org/10.1016/S1388-1981(01)00086-5).
- 24 Benito-Gallo, P., Franceschetto, A., Wong, J.C.M., Marlow, M., Zann, V., Scholes, P.,
25 Gershkovich, P., 2015. Chain length affects pancreatic lipase activity and the extent
26 and pH–time profile of triglyceride lipolysis. *European Journal of Pharmaceutics and*

- 1 Biopharmaceutics 93, 353-362. <https://doi.org/10.1016/j.ejpb.2015.04.027>.
- 2 Benito-Gallo, P., Marlow, M., Zann, V., Scholes, P., Gershkovich, P., 2016. Linking in
3 Vitro Lipolysis and Microsomal Metabolism for the Quantitative Prediction of Oral
4 Bioavailability of BCS II Drugs Administered in Lipidic Formulations. *Molecular*
5 *Pharmaceutics* 13, 3526-3540. <https://doi.org/10.1021/acs.molpharmaceut.6b00597>.
- 6 Benzonana, G., Desnuelle, P., 1965. Kinetic study of the action of pancreatic lipase on
7 emulsified triglycerides. Enzymology assay in heterogeneous medium. *Biochimica et*
8 *Biophysica Acta* 105, 121-136. <https://pubmed.ncbi.nlm.nih.gov/5849108/>.
- 9 Bhattacharjee, S., 2016. DLS and zeta potential – What they are and what they are
10 not? *Journal of Controlled Release* 235, 337-351.
11 <https://doi.org/10.1016/j.jconrel.2016.06.017>.
- 12 Carrière, F., 2016. Impact of gastrointestinal lipolysis on oral lipid-based formulations
13 and bioavailability of lipophilic drugs. *Biochimie* 125, 297-305.
14 <https://doi.org/10.1016/j.biochi.2015.11.016>.
- 15 Chen, K.-A., Farrar, M., Cardamone, M., Gill, D., Smith, R., Cowell, C.T., Truong, L.,
16 Lawson, J.A., 2018. Cannabidiol for treating drug-resistant epilepsy in children: the
17 New South Wales experience. *Medical Journal of Australia* 209, 217-221.
18 <https://doi.org/10.5694/mja18.00023>.
- 19 Cho, H.-Y., Lee, T., Yoon, J., Han, Z., Rabie, H., Lee, K.-B., Su, W.W., Choi, J.-W.,
20 2018. Magnetic Oleosome as a Functional Lipophilic Drug Carrier for Cancer Therapy.
21 *ACS Applied Materials & Interfaces* 10, 9301-9309.
22 <https://doi.org/10.1021/acsami.7b19255>.
- 23 Chu, Y., Wong, A., Chen, H., Ji, L., Qin, C., Feng, W., Stocks, M.J., Gershkovich, P.,
24 2023. Development of lipophilic ester prodrugs of dolutegravir for intestinal lymphatic
25 transport. *European Journal of Pharmaceutics and Biopharmaceutics* 191, 90-102.
26 <https://doi.org/10.1016/j.ejpb.2023.08.015>.
- 27 Couêdelo, L., Amara, S., Lecomte, M., Meugnier, E., Monteil, J., Fonseca, L., Pineau,
28 G., Cansell, M., Carriere, F., Michalski, M.-C., 2015. Impact of various emulsifiers on
29 ALA bioavailability and chylomicron synthesis through changes in gastrointestinal
30 lipolysis. *Food & function* 6, 1726-1735. <https://doi.org/10.1039/C5FO00070J>.
- 31 Court, M.H., Mealey, K.L., Burke, N.S., Jimenez, T.P., Zhu, Z., Wakshlag, J.J., 2024.
32 Cannabidiol and cannabidiolic acid: Preliminary in vitro evaluation of metabolism and
33 drug–drug interactions involving canine cytochrome P - 450, UDP -
34 glucuronosyltransferase, and P - glycoprotein. *Journal of Veterinary Pharmacology*
35 *and Therapeutics* 47, 1-13. <https://doi.org/10.1111/jvp.13403>.
- 36 Dahan, A., Hoffman, A., 2008. Rationalizing the selection of oral lipid based drug
37 delivery systems by an in vitro dynamic lipolysis model for improved oral bioavailability
38 of poorly water soluble drugs. *Journal of Controlled Release* 129, 1-10.
39 <https://doi.org/10.1016/j.jconrel.2008.03.021>.
- 40 De Chirico, S., di Bari, V., Foster, T., Gray, D., 2018. Enhancing the recovery of oilseed
41 rape seed oil bodies (oleosomes) using bicarbonate-based soaking and grinding
42 media. *Food Chemistry* 241, 419-426.
43 <https://doi.org/10.1016/j.foodchem.2017.09.008>.
- 44 Deleu, M., Vaca-Medina, G., Fabre, J.-F., Roïz, J., Valentin, R., Mouloungui, Z., 2010.

- 1 Interfacial properties of oleosins and phospholipids from rapeseed for the stability of
2 oil bodies in aqueous medium. *Colloids and Surfaces B: Biointerfaces* 80, 125-132.
3 <https://doi.org/10.1016/j.colsurfb.2010.05.036>.
- 4 Ding, J., Dong, Y., Huang, G., Zhang, Y., Jiang, L., Sui, X., 2021. Fabrication and
5 characterization of β -carotene emulsions stabilized by soy oleosin and lecithin
6 mixtures with a composition mimicking natural soy oleosomes. *Food & Function* 12,
7 10875-10886. <https://doi.org/10.1039/D1FO01462E>.
- 8 Ding, J., Wen, J., Wang, J., Tian, R., Yu, L., Jiang, L., Zhang, Y., Sui, X., 2020. The
9 physicochemical properties and gastrointestinal fate of oleosomes from non-heated
10 and heated soymilk. *Food Hydrocolloids* 100, 105418.
11 <https://doi.org/10.1016/j.foodhyd.2019.105418>.
- 12 Fallingborg, J., 1999. Intraluminal pH of the human gastrointestinal tract. *Danish*
13 *medical bulletin* 46, 183-196. <https://pubmed.ncbi.nlm.nih.gov/10421978/>.
- 14 Faul, F., Erdfelder, E., Lang, A.-G., Buchner, A., 2007. G* Power 3: A flexible statistical
15 power analysis program for the social, behavioral, and biomedical sciences. *Behavior*
16 *research methods* 39, 175-191.
- 17 Feeney, O.M., Crum, M.F., McEvoy, C.L., Trevaskis, N.L., Williams, H.D., Pouton, C.W.,
18 Charman, W.N., Bergström, C.A., Porter, C.J., 2016. 50 years of oral lipid-based
19 formulations: provenance, progress and future perspectives. *Advanced drug delivery*
20 *reviews* 101, 167-194. <https://doi.org/10.1016/j.addr.2016.04.007>.
- 21 Feng, W., Qin, C., Abdelrazig, S., Bai, Z., Raji, M., Darwish, R., Chu, Y., Ji, L., Gray,
22 D.A., Stocks, M.J., Constantinescu, C.S., Barrett, D.A., Fischer, P.M., Gershkovich, P.,
23 2022. Vegetable oils composition affects the intestinal lymphatic transport and
24 systemic bioavailability of co-administered lipophilic drug cannabidiol. *International*
25 *Journal of Pharmaceutics* 624, 121947.
26 <https://doi.org/10.1016/j.ijpharm.2022.121947>.
- 27 Feng, W., Qin, C., Chu, Y., Berton, M., Lee, J.B., Zgair, A., Bettonte, S., Stocks, M.J.,
28 Constantinescu, C.S., Barrett, D.A., Fischer, P.M., Gershkovich, P., 2021a. Natural
29 sesame oil is superior to pre-digested lipid formulations and purified triglycerides in
30 promoting the intestinal lymphatic transport and systemic bioavailability of cannabidiol.
31 *European Journal of Pharmaceutics and Biopharmaceutics* 162, 43-49.
32 <https://doi.org/10.1016/j.ejpb.2021.02.013>.
- 33 Feng, W., Qin, C., Cipolla, E., Lee, J.B., Zgair, A., Chu, Y., Ortori, C.A., Stocks, M.J.,
34 Constantinescu, C.S., Barrett, D.A., Fischer, P.M., Gershkovich, P., 2021b. Inclusion of
35 Medium-Chain Triglyceride in Lipid-Based Formulation of Cannabidiol Facilitates
36 Micellar Solubilization In Vitro, but In Vivo Performance Remains Superior with Pure
37 Sesame Oil Vehicle. *Pharmaceutics* 13, 1349.
38 <https://doi.org/10.3390/pharmaceutics13091349>.
- 39 Franco, V., Gershkovich, P., Perucca, E., Bialer, M., 2020. The interplay between liver
40 first-pass effect and lymphatic absorption of cannabidiol and its implications for
41 cannabidiol oral formulations. *Clinical Pharmacokinetics* 59, 1493-1500.
42 <https://doi.org/10.1007/s40262-020-00931-w>.
- 43 Gershkovich, P., Hoffman, A., 2005. Uptake of lipophilic drugs by plasma derived
44 isolated chylomicrons: Linear correlation with intestinal lymphatic bioavailability.

- 1 European Journal of Pharmaceutical Sciences 26, 394-404.
2 <https://doi.org/10.1016/j.ejps.2005.07.011>.
- 3 Gershkovich, P., Sivak, O., Contreras-Whitney, S., Darlington, J.W., Wasan, K.M.,
4 2012. Assessment of Cholesterol Absorption Inhibitors Nanostructured Aluminosilicate
5 and Cholestyramine Using In Vitro Lipolysis Model. Journal of Pharmaceutical
6 Sciences 101, 291-300. <https://doi.org/10.1002/jps.22770>.
- 7 Hauss, D.J., 2007. Oral lipid-based formulations. Advanced drug delivery reviews 59,
8 667-676. <https://doi.org/10.1016/j.addr.2007.05.006>.
- 9 Hess, E.J., Moody, K.A., Geffrey, A.L., Pollack, S.F., Skirvin, L.A., Bruno, P.L., Paolini,
10 J.L., Thiele, E.A., 2016. Cannabidiol as a new treatment for drug - resistant epilepsy
11 in tuberous sclerosis complex. Epilepsia 57, 1617-1624.
12 <https://doi.org/10.1111/epi.13499>.
- 13 Hoffenberg, E.J., McWilliams, S., Mikulich-Gilbertson, S., Murphy, B., Hoffenberg, A.,
14 Hopfer, C.J., 2019. Cannabis Oil Use by Adolescents and Young Adults With
15 Inflammatory Bowel Disease. Journal of Pediatric Gastroenterology and Nutrition 68.
16 <https://doi.org/10.1097/mpg.0000000000002189>
- 17 Jiang, R., Yamaori, S., Takeda, S., Yamamoto, I., Watanabe, K., 2011. Identification of
18 cytochrome P450 enzymes responsible for metabolism of cannabidiol by human liver
19 microsomes. Life Sciences 89, 165-170. <https://doi.org/10.1016/j.lfs.2011.05.018>.
- 20 Jolivet, P., Aymé, L., Giuliani, A., Wien, F., Chardot, T., Gohon, Y., 2017. Structural
21 proteomics: Topology and relative accessibility of plant lipid droplet associated proteins.
22 Journal of Proteomics 169, 87-98. <https://doi.org/10.1016/j.jprot.2017.09.005>.
- 23 Kalepu, S., Manthina, M., Padavala, V., 2013. Oral lipid-based drug delivery systems—
24 an overview. Acta Pharmaceutica Sinica B 3, 361-372.
25 <https://doi.org/10.1016/j.apsb.2013.10.001>.
- 26 Kaszuba, M., Corbett, J., Watson, F.M., Jones, A., 2010. High-concentration zeta
27 potential measurements using light-scattering techniques. Philosophical Transactions
28 of the Royal Society A: Mathematical, Physical and Engineering Sciences 368, 4439-
29 4451. <https://doi.org/10.1098/rsta.2010.0175>.
- 30 Márquez-Ruiz, G., García-Martínez, M., Holgado, F., 2008. Changes and effects of
31 dietary oxidized lipids in the gastrointestinal tract. Lipid Insights 2, LPI. S904.
32 <https://doi.org/10.4137/LPI.S904>.
- 33 Martin-Rubio, A.S., Sopelana, P., Guillén, M., 2019. The key role of ovalbumin in lipid
34 bioaccessibility and oxidation product profile during the in vitro digestion of slightly
35 oxidized soybean oil. Food & Function 10, 4440-4451.
36 <https://doi.org/10.1039/C9FO00598F>.
- 37 McClements, D.J., 2018. Enhanced delivery of lipophilic bioactives using emulsions: a
38 review of major factors affecting vitamin, nutraceutical, and lipid bioaccessibility. Food
39 & Function 9, 22-41. <https://doi.org/10.1039/c7fo01515a>.
- 40 McConnell, E.L., Basit, A.W., Murdan, S., 2008. Measurements of rat and mouse
41 gastrointestinal pH, fluid and lymphoid tissue, and implications for in - vivo
42 experiments. Journal of Pharmacy and Pharmacology 60, 63-70.
43 <https://doi.org/10.1211/jpp.60.1.0008>.
- 44 Mechoulam, R., Parker, L.A., Gallily, R., 2002. Cannabidiol: an overview of some

- 1 pharmacological aspects. *The Journal of Clinical Pharmacology* 42, 11S-19S.
2 <https://doi.org/10.1002/j.1552-4604.2002.tb05998.x>.
- 3 Muresan, P., Woodhams, S., Smith, F., Taresco, V., Shah, J., Wong, M., Chapman, V.,
4 Smith, S., Hathway, G., Rahman, R., Gershkovich, P., Marlow, M., 2023. Evaluation of
5 cannabidiol nanoparticles and nanoemulsion biodistribution in the central nervous
6 system after intrathecal administration for the treatment of pain. *Nanomedicine:*
7 *Nanotechnology, Biology and Medicine* 49, 102664.
8 <https://doi.org/10.1016/j.nano.2023.102664>.
- 9 Nichols, J.M., Kaplan, B.L.F., 2019. Immune Responses Regulated by Cannabidiol.
10 *Cannabis and Cannabinoid Research* 5, 12-31.
11 <https://doi.org/10.1089/can.2018.0073>.
- 12 Nieva-Echevarría, B., Goicoechea, E., Guillén, M.D., 2020. Food lipid oxidation under
13 gastrointestinal digestion conditions: A review. *Critical Reviews in Food Science and*
14 *Nutrition* 60, 461-478. <https://doi.org/10.1080/10408398.2018.1538931>.
- 15 Nikiforidis, C.V., 2019. Structure and functions of oleosomes (oil bodies). *Advances in*
16 *Colloid and Interface Science* 274, 102039.
17 <https://doi.org/10.1016/j.cis.2019.102039>.
- 18 Perucca, E., Bialer, M., 2020. Critical Aspects Affecting Cannabidiol Oral Bioavailability
19 and Metabolic Elimination, and Related Clinical Implications. *CNS Drugs* 34, 795-800.
20 <https://doi.org/10.1007/s40263-020-00741-5>.
- 21 Porter, C.J., Trevaskis, N.L., Charman, W.N., 2007. Lipids and lipid-based formulations:
22 optimizing the oral delivery of lipophilic drugs. *Nature reviews Drug discovery* 6, 231-
23 248. <https://doi.org/10.1038/nrd2197>.
- 24 Porter, C.J., Williams, H.D., Trevaskis, N.L., 2013. Recent advances in lipid-based
25 formulation technology. *Pharmaceutical research* 30, 2971-2975.
26 <https://doi.org/10.1007/s11095-013-1229-7>.
- 27 Qin, C., Chu, Y., Feng, W., Fromont, C., He, S., Ali, J., Lee, J.B., Zgair, A., Berton, M.,
28 Bettonte, S., Liu, R., Yang, L., Monmaturapoj, T., Medrano-Padial, C., Ugalde, A.A.R.,
29 Vetrugno, D., Ee, S.Y., Sheriston, C., Wu, Y., Stocks, M.J., Fischer, P.M., Gershkovich,
30 P., 2021. Targeted delivery of lopinavir to HIV reservoirs in the mesenteric lymphatic
31 system by lipophilic ester prodrug approach. *Journal of Controlled Release* 329, 1077-
32 1089. <https://doi.org/10.1016/j.jconrel.2020.10.036>.
- 33 Romero-Guzmán, M.J., Jung, L., Kyriakopoulou, K., Boom, R.M., Nikiforidis, C.V.,
34 2020. Efficient single-step rapeseed oleosome extraction using twin-screw press.
35 *Journal of Food Engineering* 276, 109890.
36 <https://doi.org/10.1016/j.jfoodeng.2019.109890>.
- 37 Salvia-Trujillo, L., Qian, C., Martín-Belloso, O., McClements, D.J., 2013a. Influence of
38 particle size on lipid digestion and β -carotene bioaccessibility in emulsions and
39 nanoemulsions. *Food Chemistry* 141, 1472-1480.
40 <https://doi.org/10.1016/j.foodchem.2013.03.050>.
- 41 Salvia-Trujillo, L., Qian, C., Martín-Belloso, O., McClements, D.J., 2013b. Influence of
42 particle size on lipid digestion and β -carotene bioaccessibility in emulsions and
43 nanoemulsions. *Food Chem* 141, 1472-1480.
44 <https://doi.org/10.1016/j.foodchem.2013.03.050>.

- 1 Salvia-Trujillo, L., Verkempinck, S., Sun, L., Van Loey, A., Grauwet, T., Hendrickx, M.,
2 2017. Lipid digestion, micelle formation and carotenoid bioaccessibility kinetics:
3 Influence of emulsion droplet size. *Food Chemistry* 229, 653-662.
4 <https://doi.org/10.1016/j.foodchem.2017.02.146>.
- 5 Seltzer, E.S., Watters, A.K., MacKenzie, D., Granat, L.M., Zhang, D., 2020.
6 Cannabidiol (CBD) as a promising anti-cancer drug. *Cancers* 12, 3203.
7 <https://doi.org/10.3390/cancers12113203>.
- 8 The American Oil Chemists' Society, 2011. Peroxide Value Acetic Acid-Isooctane
9 Method, Official Methods and Recommended Practices of the AOCS. The American
10 Oil Chemists' Society. [https://www.aocs.org/attain-lab-
11 services/methods/methods/search-results?method=111547](https://www.aocs.org/attain-lab-services/methods/methods/search-results?method=111547).
- 12 Tzen, J.T., Huang, A.H., 1992. Surface structure and properties of plant seed oil bodies.
13 *Journal of Cell Biology* 117, 327-335. <https://doi.org/10.1083/jcb.117.2.327>.
- 14 White, D.A., Fisk, I.D., Makkhun, S., Gray, D.A., 2009. In vitro assessment of the
15 bioaccessibility of tocopherol and fatty acids from sunflower seed oil bodies. *Journal*
16 *of Agricultural and Food Chemistry* 57, 5720-5726. <https://doi.org/10.1021/jf9003412>.
- 17 Yao, M., Kitamura, F., Han, Y., Du, H., McClements, D.J., Xiao, H., 2022. Adverse
18 effects of linoleic acid: Influence of lipid oxidation on lymphatic transport of citrus
19 flavonoid and enterocyte morphology. *Food Chemistry* 369, 130968.
20 <https://doi.org/10.1016/j.foodchem.2021.130968>.
- 21 Yi, J., Li, Y., Zhong, F., Yokoyama, W., 2014. The physicochemical stability and in vitro
22 bioaccessibility of beta-carotene in oil-in-water sodium caseinate emulsions. *Food*
23 *Hydrocolloids* 35, 19-27. <https://doi.org/10.1016/j.foodhyd.2013.07.025>.
- 24 Zgair, A., Lee, J.B., Wong, J., Taha, D.A., Aram, J., Di Virgilio, D., McArthur, J.W.,
25 Cheng, Y.-K., Hennig, I.M., Barrett, D.A., 2017. Oral administration of cannabis with
26 lipids leads to high levels of cannabinoids in the intestinal lymphatic system and
27 prominent immunomodulation. *Scientific reports* 7, 1-12.
28 <https://doi.org/10.1038/s41598-017-15026-z>
- 29 Zgair, A., Wong, J.C., Lee, J.B., Mistry, J., Sivak, O., Wasan, K.M., Hennig, I.M., Barrett,
30 D.A., Constantinescu, C.S., Fischer, P.M., Gershkovich, P., 2016. Dietary fats and
31 pharmaceutical lipid excipients increase systemic exposure to orally administered
32 cannabis and cannabis-based medicines. *Am J Transl Res* 8, 3448-3459.
33 <http://www.ncbi.nlm.nih.gov/pmc/articles/pmc5009397/>.
- 34 Zgair, A., Wong, J.C.M., Sabri, A., Fischer, P.M., Barrett, D.A., Constantinescu, C.S.,
35 Gershkovich, P., 2015. Development of a simple and sensitive HPLC–UV method for
36 the simultaneous determination of cannabidiol and Δ^9 -tetrahydrocannabinol in rat
37 plasma. *Journal of Pharmaceutical and Biomedical Analysis* 114, 145-151.
38 <https://doi.org/10.1016/j.jpba.2015.05.019>.
- 39
40
41
42
43
44

1 **Captions to Figures**

2
3 **Figure 1.** 2D structure of Cannabidiol (Created by ChemDraw, Revvity Signals
4 Software, Waltham, Ma, US)

5
6 **Figure 2.** Particle volume distribution and zeta-potential of rapeseed oleosomes and
7 artificial emulsion before and after CBD loading (n=3). A, volume distribution of
8 rapeseed oleosomes and artificial emulsion; B, volume distribution of CBD-loaded
9 rapeseed oleosomes and artificial emulsion; C, Zeta-potential of rapeseed
10 oleosomes and artificial emulsion; D, Zeta-potential of CBD-loaded rapeseed
11 oleosomes and artificial emulsion. Unpaired t test was used for analysis of
12 differences in zeta potential values between artificial emulsion and rapeseed
13 oleosomes at the same pH with or without CBD. It was found that almost all zeta
14 potential values of artificial emulsion have significant differences compared with
15 rapeseed oleosomes, except CBD-loaded artificial emulsion and CBD-loaded
16 rapeseed oleosomes at pH 8. P < 0.05 was considered statistically significantly
17 different.

18 **Figure 3.** CBD partitioning into lipid, micellar aqueous, and sediment phases after *in*
19 *vitro* lipolysis of CBD-loaded rapeseed oil, rapeseed oleosomes and artificial
20 emulsion. (mean ± SD, n = 3). One-way ANOVA, followed by Tukey 's multiple
21 comparisons test was applied to evaluate the statistical significance of differences
22 between means of CBD distribution into three phases. *, p < 0.05, ****, p < 0.0001.

23 **Figure 4.** Peroxide value for different rapeseed-based formulations (Mean ± SD,
24 n=3). ****, P < 0.0001. One-way ANOVA, followed by Tukey 's multiple comparisons
25 test was applied to evaluate the statistical significance of differences between
26 means.

27 **Figure 5.** Plasma CBD concentrations-time profile following oral administration of 3
28 mg/kg CBD in different formulations in Sprague Dawley rats (Mean ± SD, n = 5/6).

29 **Figure 6.** Biodistribution of CBD at plasma t_{max} and t_{max} -1h following oral
30 administration of 3 mg/kg CBD in different formulations in Sprague Dawley rats
31 (Mean ± SD, n = 4). MLN, mesenteric lymph nodes. A, biodistribution of CBD at
32 plasma t_{max} ; B, biodistribution of CBD at plasma t_{max} -1h. One-way ANOVA, followed
33 by Tukey 's multiple comparisons test was applied to evaluate the statistical
34 significance of differences between means. *, p < 0.05, **, p < 0.01.

35